Different Murine High-Risk Corneal Transplant Settings Vary Significantly in Their (Lymph)angiogenic and Inflammatory Cell Signatures

Wei Zhang,[1] Alfrun Schönberg,[1] Fiona Bassett,[1] Karina Hadrian,[1] Deniz Hos,[1] Martina Becker,[1] Felix Bock,[1,2] and Claus Cursiefen[1,2]

[1]Department of Ophthalmology, Faculty of Medicine and University Hospital Cologne, University of Cologne, Cologne, Germany
[2]Center for Molecular Medicine Cologne (CMMC), University of Cologne, Cologne, Germany

Correspondence: Felix Bock, University of Cologne, Faculty of Medicine and University Hospital Cologne, CorneaLab, Experimental Ophthalmology, LFI Building 13, University Hospital of Cologne, Kerpener Strasse 62, Cologne 50924, Germany; felix.bock@uk-koeln.de.

Claus Cursiefen and Felix Bock are co-senior authors.

Received: August 2, 2022
Accepted: November 30, 2022
Published: December 19, 2022

Citation: Zhang W, Schönberg A, Bassett F, et al. Different murine high-risk corneal transplant settings vary significantly in their (lymph)angiogenic and inflammatory cell signatures. *Invest Ophthalmol Vis Sci.* 2022;63(13):18. https://doi.org/10.1167/iovs.63.13.18

Purpose. Pathologic conditions in the cornea, such as transplant rejection or trauma, can lead to corneal neovascularization, creating a high-risk environment that may compromise subsequent transplantation. This study aimed to evaluate the impact of different types of corneal injury on hemangiogenesis (HA), lymphangiogenesis (LA) and immune cell pattern in the cornea.

Methods. We used five different corneal injury models, namely, incision injury, alkali burn, suture placement, and low-risk keratoplasty, as well as high-risk keratoplasty and naïve corneas as control. One week after incision and 2 weeks after all other different injuries, corneal HA and LA were quantified by morphometric analysis. In addition, immune cell patterns of the whole cornea and the recipient rim were analyzed by immunohistochemistry. Immune cells in the draining lymph nodes (dLNs) were quantified by flow cytometry.

Results. Different types of corneal injury caused significantly different HA and LA responses (both $P < 0.0001$). The infiltration of corneal macrophages, dendritic cells, neutrophils, major histocompatibility complex (MHC) II$^+$ cells, CD4$^+$ T cells, and CD8$^+$ T cells varied significantly in different high-risk settings (all $P < 0.0001$). Both the expression of MHC II on macrophages ($P = 0.0005$) and the frequency of MHC II$^+$ dendritic cells ($P = 0.0014$) in the draining lymph nodes were significantly different across the various high-risk scenarios.

Conclusions. Murine high-risk settings caused by different underlying pathologies vary significantly in their (lymph)angiogenic and inflammatory cell patterns. Therefore, anti(lymph)angiogenic or immunomodulatory strategies to prevent and/or treat immune responses after subsequent corneal transplantation may need to be customized according to their immune-vascular "signatures."

Keywords: corneal transplantation, corneal injury, hemangiogenesis, lymphangiogenesis, inflammatory cells, macrophages, immunohistochemistry

The cornea is the transparent windshield of the eye. It is the optically most relevant refractive structure of the eye.[1] The cornea's transparency is essential for good vision and is highly conserved in evolution.[2,3] Different corneal diseases can lead to loss of transparency and corneal transplantation is the primary treatment for restoring vision. More than 50,000 corneal transplantations are performed annually in Europe, with more than 8000 transplants in Germany.[4] Whereas in industrialized countries, more and more transplantations are lamellar, a large proportion of penetrating keratoplasty are still performed worldwide.[5] Although the early outcomes of corneal allotransplantation are typically excellent (90% at 1 year after surgery), the survival of penetrating corneal allografts after 15 years decreases to 55%.[6] This rate is drastically decreased if the recipient cornea is inflamed and vascularized and, therefore, represents a high-risk situation.[6]

Reasons for corneal inflammation and neovascularization are manifold, including infection, physical trauma, chemical burn, and graft rejection.[7,8] Approximately 40% of the first graft rejections, 68% of the second graft rejections, and 81% of the third graft rejections occur in patients with a vascularized recipient bed.[9] Graft rejection rates are increased because of immune memory, presensitization, and/or a fast recognition by the host's immune response.[9] Moreover, the presence of active inflammation and infection during surgery ("hot grafting") considerably increases the risk of corneal allograft rejection and graft failure owing to nonimmunologic factors.[7,10] A majority of clinical studies have shown that irreversible rejection is the most important cause of corneal graft failure after transplantation.[11,12]

Presently, there is limited information about the recruitment of immune cells, as well as the induction of hemangiogenesis (HA) and lymphangiogenesis (LA) in different

preoperative settings, leading to a subsequent high-risk scenario in corneal transplantation. Therefore, this study aimed to characterize a broad panel of commonly used murine injury models leading to a high-risk setting with respect to their immune cells, as well as hemangiogenic and lymphangiogenic phenotypes.

Material and Methods

Animals and Anesthesia

Female BALB/c (Fig. 1A) and C57BL/6N mice (6–8 weeks old) were purchased from Charles River Laboratories (Sulzfeld, Germany). Surgical interventions were performed after deep intraperitoneal anesthesia with 8 mg/kg Ketanest (Godecke AG, Karlsruhe, Germany) and 0.1 mL/kg Rompun (Bayer, Leverkusen, Germany). The experiments were approved by the State Agency for Nature, Environment and Consumer Protection NRW and are in line with the guidelines of the ARVO Statement for the Use of Animals in Ophthalmologic and Visual Research.

Incision Model

The incision model was performed as described before.[13] In brief, one drop of atropine sulfate (1%, Ursapharm GmbH, Saarbrücken, Germany) was administrated to induce mydriasis. The central cornea was marked with a 1.0-mm trephine after full corneal penetration using a 30G needle and a sagittal linear perforating incision with surgical micro scissors (Fig. 1B).

Alkali Burn Model

The alkali burn model was performed as described before.[14] In brief, a 2.0-mm filter disc soaked in 1 M NaOH was placed on the central corneal surface for 30 seconds, and the eyes were washed immediately with PBS for 2 minutes (Fig. 1C).

Suture Model

The suture model was performed as described before.[15–17] In brief, three interrupted figure-of-eight sutures (11-0 nylon, Serag-Wiessner, Naila, Germany) were placed in the cornea's stroma and left in place for 14 days. On day 14, the sutures were removed and animals were either sacrificed or used for subsequent high-risk transplantation (Fig. 1D).

Low-Risk and High-Risk Keratoplasty (HR-KPL) Model

Naïve BALB/c mice served as low-risk recipients. For the high-risk condition, sutures were placed as described elsewhere in this article in BALB/c mice and removed after 14 days before corneal transplantation. Keratoplasty was performed as described previously.[5,12,18] Age-matched C57BL/6 mice served as donors. Donor corneas (Ø = 2 mm) were excised by trephination, placed in the recipient's bed and secured with eight interrupted sutures (11-0 nylon, Serag-Wiessner) (Figs. 1E, 1F). Seven days after transplantation, sutures holding the corneal graft in place were removed.

Immunohistochemistry and Morphological Analysis of HA and LA in Corneal Whole-mounts

One week after incision injury and 2 weeks after alkali burn, suture, low-risk/HR-KPL ($n = 5$, naïve corneas as control), corneas were excised to quantify blood vessels (BVs) and lymphatic vessels (LVs) as previously described.[16,19,20] Briefly, corneal whole-mounts were stained with CD31 (Table) for BVs and LYVE-1 (Table) for LVs. Subsequently, sections were analyzed using fluorescence microscopy (BX53, Olympus, Hamburg, Germany). Finally, as previously described, the percentages of BVs and LVs covering the cornea were evaluated using CellˆF (Olympus, Germany).[21–23]

Immune Cell Counting in Corneas

In each model, five eyeballs were used for cryosections (6 µm). Sections were stained with antibodies against Ly6G, F4/80, CD11c, major histocompatibility complex (MHC) II, CD3, CD4, and CD8 (Table). Images were acquired using a fluorescence microscope (BX53, Olympus). Areas covered by positive cells were measured using CellˆF. Briefly, the complete corneal border was outlined as the region of interest, and stained cells were detected by setting a gray scale value threshold, including the bright cells and excluding the dark background. The percentage of the area covered by stained cells in the region of interest was calculated.

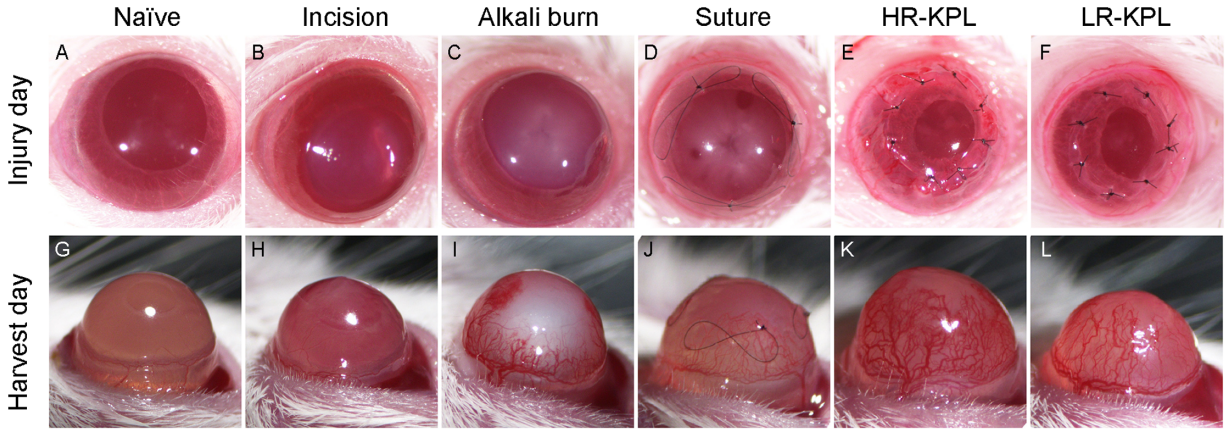

Figure 1. Images of murine corneas after different injury models leading to a "high-risk" recipient bed. Representative images of naïve cornea and five types of injury model at the injury day (**A–F**) and at the harvest day (**G–L**), (timepoint: 1 week after incision injury, 2 weeks after alkali burn, suture, HR-KPL and LR-KPL).

Investigative Ophthalmology & Visual Science

Table. List of Antibodies, Fluorochromes, Clones, Usages, and Manufacturers

Antibody	Fluorochrome	Clone	Usage	Manufacturer
Rat anti-mouse CD45	PE/Cy7	30-F11	FCM	BioLegend
Rat anti-mouse F4/80	FITC	BM8	FCM	BioLegend
Rat anti-mouse CD11b	APC/Cy7	M1/70	FCM	BioLegend
Hamster anti-mouse CD11c	PE	N418	FCM	BioLegend
Rat anti-mouse I-A/I-E (MHC II)	Pacific Blue	M5/114.15.2	FCM	BioLegend
Rat anti-mouse CD3	PE/Cy7	17A2	FCM	BioLegend
Rat anti-mouse CD4	APC	RM4-5	FCM	eBioscience
Rat anti-mouse CD8	APC/Cy7	YTS156.7.7	FCM	BioLegend
Rat anti-mouse CD16/CD32	N/A	2.4G2	Fc block	BD Bioscience
Rat anti-mouse F4/80	N/A	N/A	IF	Thermo Fisher Scientific
Hamster anti-mouse CD11c	Alexa Fluor 647	N418	IF	BioLegend
Rat anti-mouse Ly6G	Alexa Fluor 647	1A8	IF	BioLegend
Rat anti-mouse I-A/I-E (MHC II)	Alexa Fluor 488	M5/114.15.2	IF	BioLegend
Rabbit anti-mouse CD3	N/A	N/A	IF	Abcam
Rat anti-mouse CD4	N/A	GK1.5	IF	Thermo Fisher Scientific
Rat anti-mouse CD8	N/A	5H10-1	IF	BioLegend
Rat anti-mouse CD31	FITC	390	IF	BD Bioscience
Rabbit anti-mouse LYVE-1	N/A	N/A	IF	AngioBio
Goat anti-rabbit IgG (H^+L)	Alexa Fluor 488	N/A	IF	Thermo Fisher Scientific
Goat anti-rabbit IgG (H^+L)	Cy3	N/A	IF	Jackson ImmunoResearch
Goat anti-rat IgG (H^+L)	Alexa Fluor 555	N/A	IF	Thermo Fisher Scientific

APC, allophycocyanin; CD, cluster of differentiation; Cy, cyanine; FCM, flow cytometry; FITC, fluorescein isothiocyanate; IF, immunofluorescence; LYVE-1, lymphatic vessel endothelial hyaluronan receptor 1; N/A, not applicable; PE, phycoerythrin.

Optical Coherence Tomography (OCT) and Histological Analysis

To assess corneal thickness after injury, in vivo OCT of the cornea was performed for each injury model at the respective endpoint using a custom-made OCT system (PR3-13A, Thorlabs GmbH, Lübeck, Germany). In addition, paraffin sections were stained with hematoxylin and eosin and PAS staining.

Flow Cytometry

Ipsilateral submandibular lymph nodes were excised at the indicated time points after injury to prepare a single-cell suspension. After blocking with Fc block (Table), cells were stained with antibodies against CD45, F4/80, CD11b, CD11c, MHC II, CD3, CD4, and CD8 (Table). Fluorescence minus one and unstained cells were used as the gating controls. Fluorescence was measured by a flow cytometer (Canto II, BD Biosciences, Franklin Lakes, NJ, USA), and data were analyzed using FlowJo (version 10.7.1, Ashland, OR, USA).

Statistical Analysis

One-way ANOVA with Turkey's multiple comparisons was used for statistical analyses. Data were shown as mean ± standard deviation. A P value of less than 0.05 was considered statistically significant. Prism 8 version 8.2.1 (GraphPad Software, San Diego, CA, USA) was used for all statistical analyses and graphs.

Results

Injury-Specific and Variable (Lymph)Angiogenic Responses in the Cornea

Because corneal BVs and LVs are known risk factors for corneal graft rejection,[24] we first compared the induction of corneal HA and LA among different injury models (Figs. 1G–L). Here we found that different types of corneal injury caused significantly different corneal hemangiogenic and lymphangiogenic responses. The HR-KPL initiated the highest HA response in the whole cornea including graft and recipient, significantly higher than all other groups except low-risk keratoplasty (LR-KPL). LR-KPL induced the second most powerful angiogenic response, significantly higher than alkali burn, incision, and naïve eyes. Suture placement evoked the third most powerful HA response, significantly higher than alkali burn, incision, and naïve eyes. Alkali burn induced the fourth most powerful corneal neovascularization, significantly higher than incision and naïve eyes. Interestingly, the incision model did not induce any HA (Figs. 2A–F, 2M).

HR-KPL again provoked the highest response for LA, significantly higher than all other groups. LR-KPL induced the second highest lymphangiogenic response with a significant difference from all other groups except the alkali burn. LA in the alkali burn model and suture model was only significantly higher than in incision and naïve eyes. In contrast, a corneal incision in BALB/c mice provoked not significantly more LA compared with naïve corneas (Figs. 2G–L, 2N).

Because we expected a higher angiogenic response in the HR-KPL than in LR-KPL, we compared HA and LA in the central cornea (Ø = 2 mm, yellow dotted lines; Figs. 2A–L). As shown in Figures 2M and 2N, both HA and LA were significantly increased in the center of HR-KPL compared with LR-KPL ($n = 5$; BVs: $P = 0.0116$; LVs: $P < 0.0001$).

During keratoplasty, the central cornea of the recipient is removed and replaced by donor tissue. Therefore, we next analyzed the remaining peripheral recipient cornea only (Figs. 2A–L) in all injury models. In this case, HR-KPL also induced the significantly higher HA and LA responses compared with all other groups with the exception of LR-KPL. Interestingly, a similar percentage of BVs was shown between LR-KPL and suture model whereas there was no significant difference among LR-KPL, suture and alkali burn eyes in the percentage of LVs (Figs. 2M–O).

Investigative Ophthalmology & Visual Science

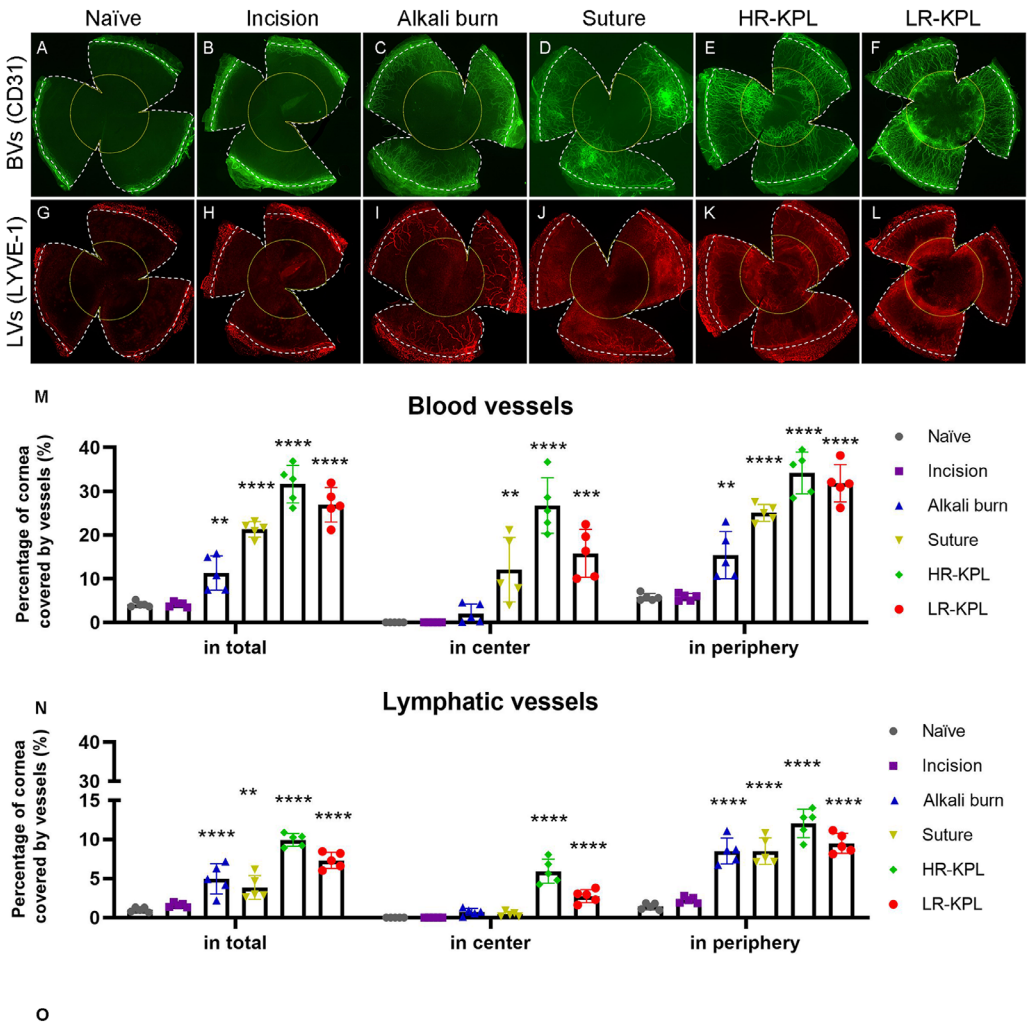

O

Tukey's multiple comparisons test	BVs in total	BVs in center	BVs in periphery	LVs in total	LVs in center	LVs in periphery
Incision vs. Alkali burn	**	ns	**	***	ns	****
Incision vs. Suture	****	**	****	*	ns	****
Incision vs. HR-KPL	****	****	****	****	****	****
Incision vs. LR-KPL	****	***	****	****	****	****
Alkali burn vs. Suture	***	*	**	ns	ns	ns
Alkali burn vs. HR-KPL	****	****	****	****	****	**
Alkali burn vs. LR-KPL	****	**	****	*	**	ns
Suture vs. HR-KPL	***	***	**	****	****	**
Suture vs. LR-KPL	ns	ns	ns	***	***	ns
HR-KPL vs. LR-KPL	ns	*	ns	*	****	ns

Figure 2. Different hemangiogenic and lymphangiogenic response patterns lead to a high-risk transplant recipient setting after different corneal injuries. (**A–L**) Representative whole-mounts of the murine corneas. BVs were stained with CD31 (*green*, **A–D**) and LVs were stained with LYVE-1 (*red*, **G–L**) (original magnification ×100; scale bar, 500 µm; total cornea, the area of white dotted lines; central cornea [Ø = 2 mm], the area of yellow lines; peripheral cornea, total cornea minus central cornea). (**M**, **N**) Percentage of BVs and LVs in total, central and peripheral cornea at harvest day ($n = 5$; *statistically significant difference of all groups compared with naïve. (**O**) Statistical results between any two groups except naive. (Timepoint: 1 week after incision injury, 2 weeks after alkali burn, suture, HR-KPL and LR-KPL.) *$P < 0.05$; **$P < 0.01$; ***$P < 0.001$; ****$P < 0.0001$. ns, not significant.

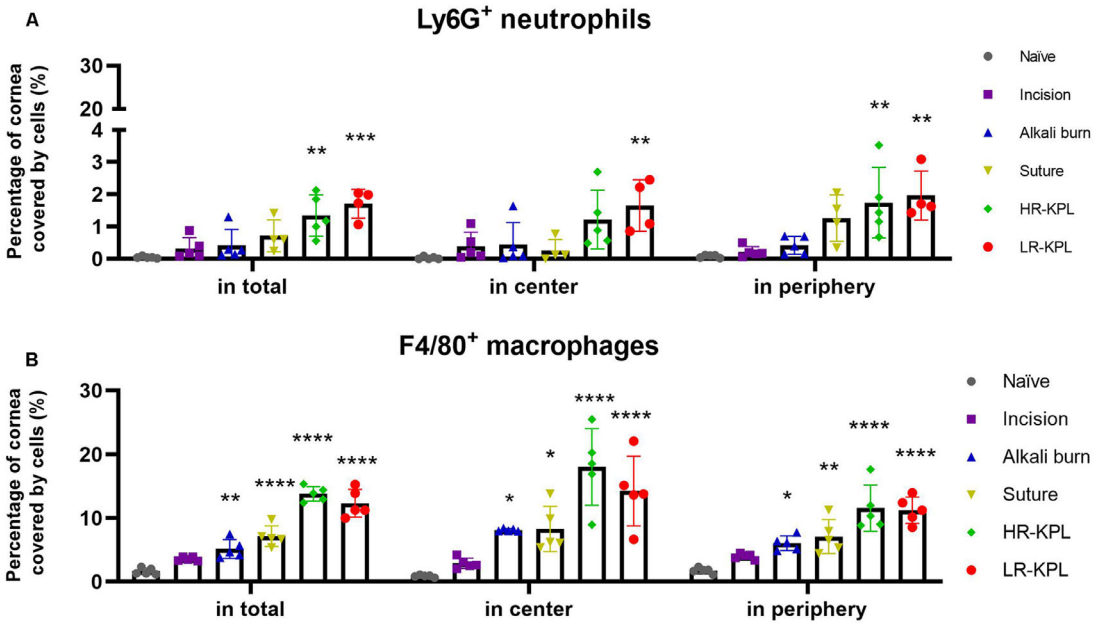

C

Tukey's multiple comparisons test	neutrophils in total	neutrophils in center	neutrophils in periphery	Mφ in total	Mφ in center	Mφ in periphery
Incision vs. Alkali burn	ns	ns	ns	ns	ns	ns
Incision vs. Suture	ns	ns	ns	**	ns	ns
Incision vs. HR-KPL	*	ns	ns	****	****	****
Incision vs. LR-KPL	**	ns	ns	****	***	***
Alkali burn vs. Suture	ns	ns	ns	ns	ns	ns
Alkali burn vs. HR-KPL	*	ns	ns	****	**	**
Alkali burn vs. LR-KPL	**	ns	ns	****	ns	**
Suture vs. HR-KPL	ns	ns	ns	****	**	*
Suture vs. LR-KPL	*	*	*	****	ns	*
HR-KPL vs. LR-KPL	ns	ns	ns	ns	ns	ns

Figure 3. Neutrophils and macrophages recruit into the cornea in different high-risk settings. (**A**, **B**) The percentage of Ly6G$^+$ neutrophils and F4/80$^+$ macrophages in total, central and peripheral corneas ($n = 5$; *statistically significant difference of all groups compared with naïve). (**C**) Statistical results between any two groups except naive. (Timepoint: 1 week after incision injury, 2 weeks after alkali burn, suture, HR-KPL and LR-KPL.) *$P < 0.05$; **$P < 0.01$; ***$P < 0.001$; ****$P < 0.0001$. ns, not significant.

Injury-Dependent Specific and Variable Immune Cell Recruitment Pattern into the Cornea

BVs and LVs contribute to graft rejection by providing invasion and evasion routes for innate and adaptive immune cell populations. In this context, we analyzed the frequency of corneal neutrophils, macrophages, dendritic cells (DCs), MHC II$^+$ cells, and T cells in different high-risk settings at the peak of corneal neovascularization (Supplementary Fig. S1; $n = 5$; $P < 0.0001$).

Neutrophils are promptly recruited after corneal injury.[25,26] Here, we show for the first time that Ly6G$^+$ neutrophils can still be found in corneas 2 weeks after HR-KPL and LR-KPL (Fig. 3A). Macrophages are the second line of defense; they are also recruited in the first 24 hours after injury[18] and remain up to 14 days after injury.[27] Although the incision trauma in BALB/c mice did not feature an increased frequency of F4/80$^+$ macrophages compared with the naïve controls, all other injuries induced significant recruitment of F4/80$^+$ macrophages, with the highest frequency observed again in HR-KPL and LR-KPL (Figs. 3B, 3C). DCs are resident in the normal corneal stroma.[28] Our laboratory has previously reported that DCs play an key role in the initiation of the adaptive immune response and in the induction of tolerance.[23,29,30] Here, we show that CD11c$^+$ DCs are only significantly increased after corneal transplantation and suture placement, whereas alkali burn induced some, but not statistically significant,

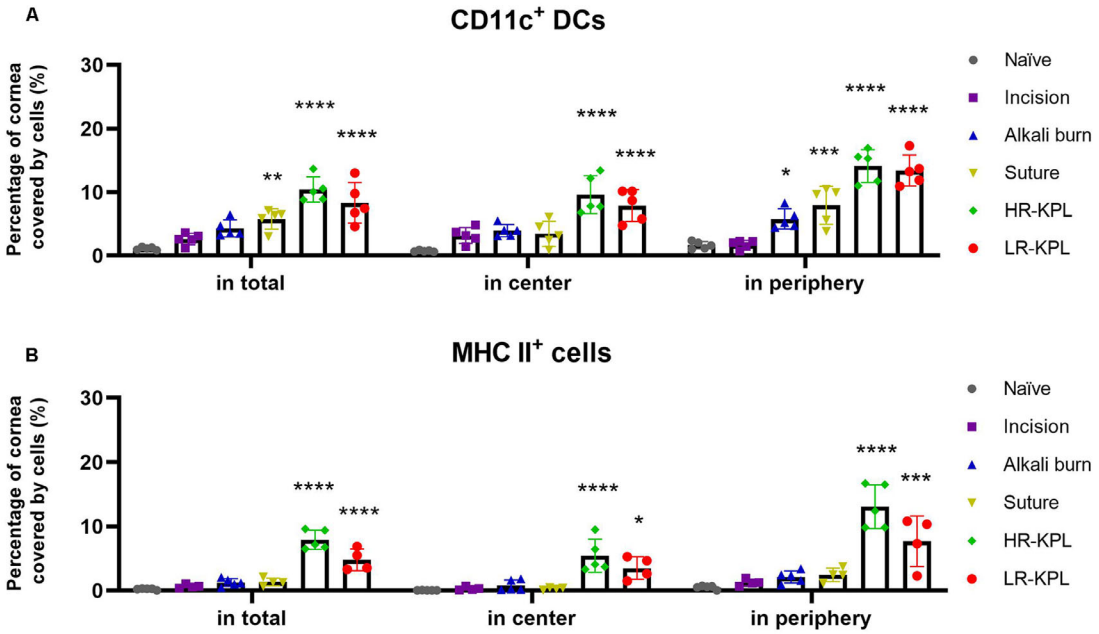

C

Tukey's multiple comparisons test	DCs in total	DCs in center	DCs in periphery	MHC II+ cells in total	MHC II+ cells in center	MHC II+ cells in periphery
Incision vs. Alkali burn	ns	ns	*	ns	ns	ns
Incision vs. Suture	ns	ns	***	ns	ns	ns
Incision vs. HR-KPL	****	***	****	****	***	****
Incision vs. LR-KPL	***	**	****	****	*	**
Alkali burn vs. Suture	ns	ns	ns	ns	ns	ns
Alkali burn vs. HR-KPL	***	**	****	****	***	****
Alkali burn vs. LR-KPL	*	*	****	***	ns	*
Suture vs. HR-KPL	**	***	***	****	***	****
Suture vs. LR-KPL	ns	*	**	***	*	*
HR-KPL vs. LR-KPL	ns	ns	ns	**	ns	*

Figure 4. DCs and MHC II$^+$ cells recruit into the cornea in high-risk settings. (**A**, **B**) Percentage of CD11c$^+$ DCs and MHC II$^+$ cells in total, central and peripheral corneas ($n = 5$; *statistically significant difference of all groups compared with naïve). (**C**) Statistical results between any two groups except naïve. (Timepoint: 1 week after incision injury, 2 weeks after alkali burn, suture, HR-KPL and LR-KPL.) *$P < 0.05$; **$P < 0.01$; ***$P < 0.001$; ****$P < 0.0001$). ns, not significant.

recruitment of DCs. The perforating injury did not result in a higher DCs frequency compared with the naïve controls (Fig. 4A). When analyzing the cells in our five injuries, only corneas after HR-KPL and LR-KPL showed a significant increased frequency of MHC II$^+$ immune cells (Figs. 4B, 4C). In corneas after HR-KPL and LR-KPL, a massive invasion of CD3$^+$, CD4$^+$, and CD8$^+$ T cells was observed, whereas in HR-KPL significantly more CD4$^+$ T cells were recruited compared with LR-KPL (Supplementary Fig. S2).

Furthermore, we analyzed the immune cell frequency separately in the peripheral and central cornea among all the injury models. Here, HR-KPL and LR-KPL showed the highest immune cell infiltration including neutrophils, macrophages, DCs, MHC II$^+$ cells, CD3$^+$ T cells, and CD4$^+$ T cells, as well as CD8$^+$ T cells in the periphery as well as in the center (Figs. 3, 4, Supplementary Fig. S2). Suture placement and alkali burn induced significantly higher macrophage and DC recruitment in the periphery compared with the naïve eyes, whereas in the central cornea these changes diminished (Figs. 4A, 4C). Incision did not induce any significant differences in the recruitment of any of the immune cells compared with naïve eyes in the periphery and the center (Figs. 3, 4).

Injury-Dependent Immune Cell Activation in the Draining Lymph Nodes (dLNs)

The dLNs reflect the immune status of the upstream tissue and play an important role in graft survival. Therefore,

Investigative Ophthalmology & Visual Science

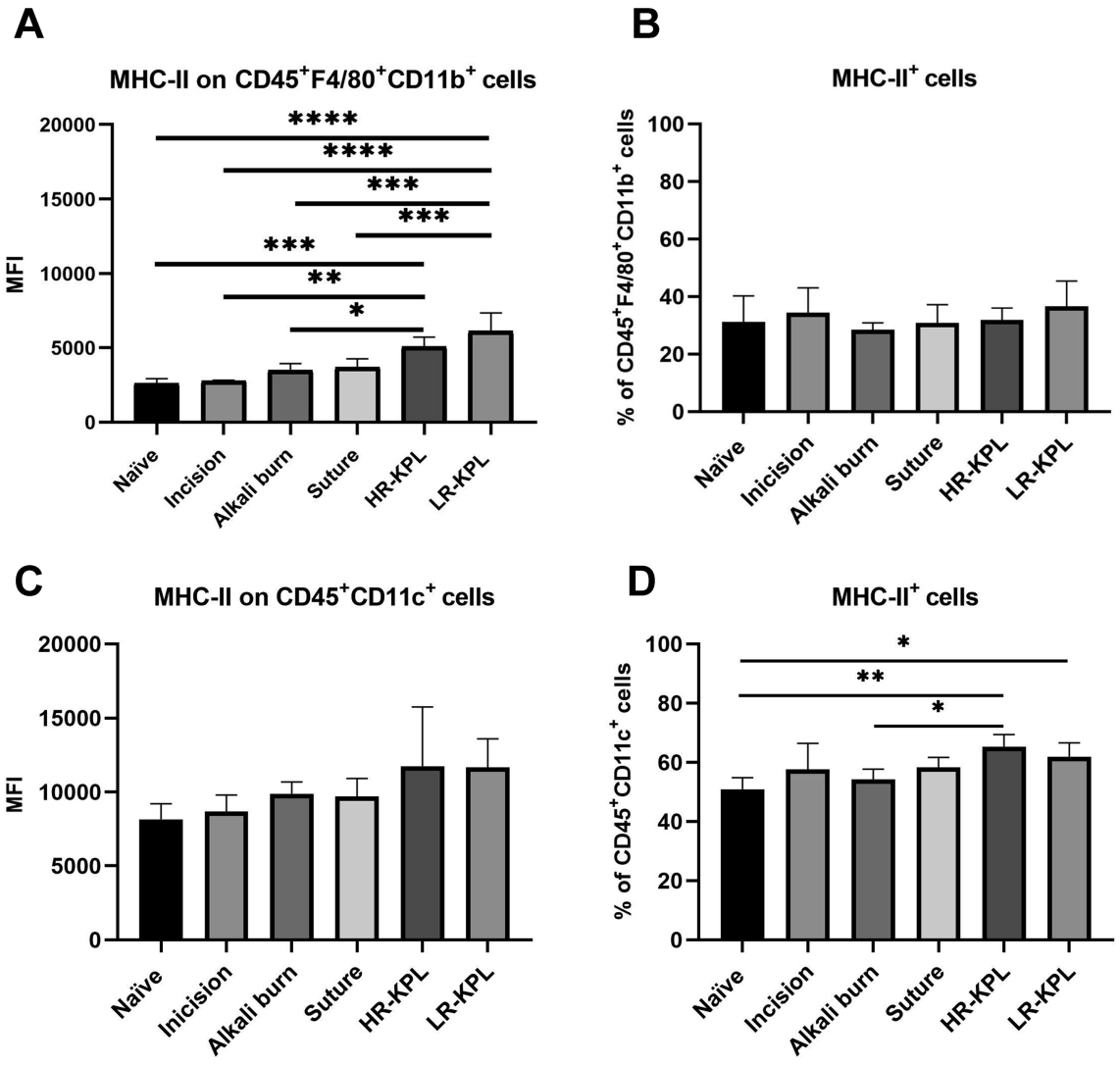

Figure 5. Disease-specific immune cell compositions in the dLNs after different corneal injuries lead to a high-risk corneal transplant setting. (**A**) MFI of MHC II on $CD45^+F4/80^+CD11b^+$ macrophages. (**B**) Frequency of MHC II^+ cells in $CD45^+F4/80^+CD11b^+$ macrophages. (**C**) MFI of MHC II on $CD45^+CD11c^+$ DCs. (**D**) Frequency of MHC II $^+$ cells (in $CD45^+CD11c^+$ DCs). (Timepoint: 1 week after incision injury, 2 weeks after alkali burn, suture, HR-KPL and LR-KPL.) $n = 5$; $^*P < 0.05$, $^{**}P < 0.01$, $^{***}P < 0.001$, $^{****}P < 0.0001$. MFI, mean fluorescence intensity.

we characterized the activated status of macrophages and DCs, because they are within the first line of recruited cells after transplantation and orchestrate the adaptive immune response. Here we found that $CD11b^+F4/80^+$ macrophages were highly MHC II positive in transplantation models in comparison to all other injury models without allogeneic stimulus (Figs. 5A, 5B). Although the MHC II expression on DCs in dLNs was not significantly increased, the frequency of $CD45^+CD11c^+$MHC II^+ DCs was significantly increased in dLNs 2 weeks after HR-KPL as well as LR-KPL, in comparison with naïve and alkali burn corneas (Figs. 5C, 5D).

Corneal Tissue Damages in Different Injury Models

In the representative central cornea of histological images from hematoxylin and eosin staining (Figs. 6A–F) and PAS staining (Figs. 6G–L), cell counts increased visually in HR-KPL and LR-KPL groups. This finding correlated with the significantly elevated influx of immune cells into the cornea in these two groups, as shown in Figures 3 and 4 and Supplementary Figure S2.

Corneal thickness is a further indicator of the inflammatory status of the cornea. Using in vivo OCT (Figs. 6M–R), we demonstrated that HR-KPL provoked the highest central corneal thickness among all groups with a significant difference ($n = 3$, Fig. 6S). Interestingly, there was no significant difference among all eyes in the mean thickness of the peripheral cornea ($n = 3$, Fig. 6T).

Discussion

In this study, we report for the first time a comparative profile of corneal hemangiogenic and lymphangiogenic as well as corneal and dLNs immune cell response patterns after different, clinically relevant murine corneal injury models. These data point to the following facts: (1) There are significant differences in hemangiogenic and lymphangiogenic responses between the different injury models (≤7-fold). This point is also true when comparing the central and

Investigative Ophthalmology & Visual Science

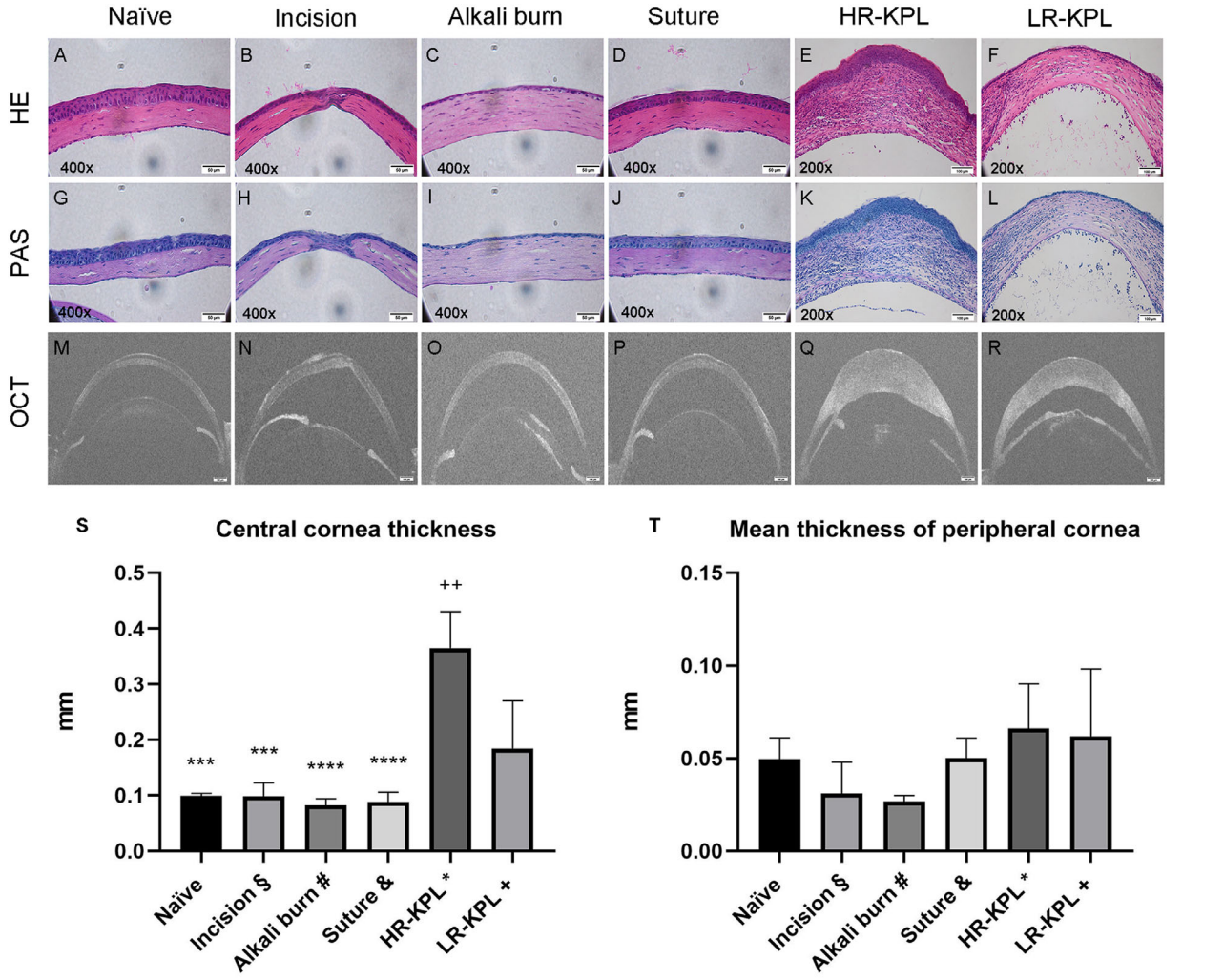

Figure 6. Different morphologic damages of the cornea among different injury models. (**A–R**) Representative central cornea with hematoxylin and eosin staining and PAS staining (**A–D** and **G–J**, original magnification ×400; scale bar, 50 µm; **E**, **F**, **K**, and **L**, original magnification ×200; scale bar, 100 µm), as well as the whole cornea OCT images (**M–R**, scale bar, 100 µm). (**S**) HR-KPL has the highest central cornea thickness (from OCT) among all the models ($n = 3$; $^{**}P < 0.01$, $^{***}P < 0.001$, $^{****}P < 0.0001$). (**H**) No significant differences were found in the mean thickness of the peripheral cornea ($n = 3$). (Three rejected corneas in HR-KPL and one rejected cornea in LR-KPL). Timepoint: 1 week after incision injury, 2 weeks after alkali burn, suture, HR-KPL and LR-KPL.

peripheral cornea. In general, LR-KPL and HR-KPL caused the most robust vascular response. (2) All disease models studied here were characterized by a parallel ingrowth of BVs and LVs into the cornea, except the incision model which induced isolated LA. (3) Up to 10-fold changes in immune cell densities after different injuries were observed. (4) MHC II^+ cells in dLNs varied up to three-fold, depending on disease entity.

Pathologic corneal neovascularization was reported to occur in 4.14% of ophthalmologic outpatients, of which 12% presented with decreased visual acuity.[31] Corneal neovascularization can be caused by different underlying pathologies.[32] In inflammatory corneal neovascularization (e.g., owing to corneal suturing[19] or after transplantation[17,37]), BVs are usually accompanied by clinically invisible LVs.[33] In contrast, in other disease settings or models, the occurrence of the two vascularization types can be unrelated. In the murine model of acute keratoconus, characterized by the acute and massive fluid influx, we recently observed isolated LA, which regressed quickly.[17] As expected in our study, keratoplasty induced the highest amounts of BVs and LVs in the whole cornea and the peripheral cornea (Figs. 2M, 2N) compared with all other injuries. Compared with incision and suture injuries, the degree of surgical trauma in keratoplasty is evidently greater. The degree of surgical trauma seems to be a significant mediator for corneal hem(lymph)angiogenesis, similar to a previous study in patients comparing different types of corneal transplant surgery techniques including mechanical versus laser trephination.[34]

After transplantation, antigen-presenting cells (APCs) from the graft can immediately migrate to the regional lymph nodes via LVs (i.e., the afferent arm), resulting in accelerated allosensitization. In this context, T cells can be activated and quickly return to the graft via preexisting BVs (i.e., the efferent arm), leading to graft rejection.[35–38] Although there was no significant difference in the overall degree of BVs in the whole cornea after HR-KPL and LR-KPL, significantly more BVs and LVs invaded into the grafts in HR-KPL than in LR-KPL (Figs. 2M, 2N), which here may contribute to the higher

transplant rejection rate. A previous study used the incision model for C57BL/6N mice to mimic acute keratoconus. Corneal incision injury caused significant LA and corneal edema but not HA.[13] In this study, we confirmed these results in the incision injury of BALB/c mice. Although it did not provoke a significant difference in BVs and LVs compared with naïve corneas among all the six groups, when only compared with the naïve eyes, the incision model of BALB/c mice initiated significantly more LVs.

It has been demonstrated that nearly all types of immune cells reside in the healthy cornea, especially those controlling innate immunity.[39–41] On the same note, our data exhibited the presence of macrophages and DCs in the naive corneas (Figs. 3, 4). A complex cascade of cellular infiltration into the cornea occurs after corneal inflammation or injury.[42–45] Subsequently, the infiltrating immune cells can secret different proinflammatory cytokines and chemokines, leading to the recruitment of more immune cells, as well as ingrowth of corneal BVs and LVs, which aim either to facilitate the healing or promote tissue damage (immune amplification cascade).[37,42,43,46,47] Macrophages and neutrophils are the two central cell populations that initiate the innate immune response with various functions, including the secretion of cytokines and lipid signaling molecules to coordinate the behavior of other immune cells.[48] After corneal injury, neutrophils are usually the first cells to infiltrate the cornea. They migrate into the corneal stroma in two waves after corneal epithelial wounding.[45] It was shown that neutrophils were present on donor endothelium after penetrating and lamellar keratoplasty in rabbits[49] and in mice.[50] Neutrophils play an important role in graft rejection and are involved in acute cellular and chronic rejection.[51] Our data show that only after HR-KPL and LR-KPL did a significant invasion of neutrophils take place, whereas after nonallospecific inflammation like suture placement or alkali burn, the neutrophil frequency was not significantly increased compared with controls. Moreover, this increase was limited to the peripheral cornea. The reason for this local limitation has to be analyzed in further studies.

Shortly after neutrophil recruitment, macrophages reach the corneal graft. Macrophages play a prominent role in inducing inflammatory corneal LA[16] and can present antigens to T cells emigrating from the vessels at the corneal limbus.[41] In our study, all types of injury significantly recruited the incidence of macrophages into the peripheral and central cornea, with the exception of the incision model. In the HR-KPL and LR-KPL models, which also comprise the greatest degree of corneal HA and LA, the greatest level of macrophage infiltration was observed, increasing the risk for allogeneic immune rejection.

An even more important immune cell subset for immune-mediated graft rejection is DCs. They are well-known central mediators of immune responses[52] and play a key role in corneal graft rejection.[53] Whereas our data showed that suture placement as well as HR-KPL and LR-KPL induced a robust, all-over invasion of DCs into the cornea, the alkali burn and incision models did not significantly increase their incidence. In contrast, DC recruitment was significantly increased in the peripheral cornea after suture placement and alkali burn compared with the controls. These data point out that DCs may be a valid target to improve high-risk graft survival, even after mild alkali burns.

In adaptive immunity, allospecific T cells are activated by APCs providing the proper peptide–MHC complex. Rejected corneal transplants from both humans and animals show mixed inflammatory infiltrates including both $CD4^+$ and $CD8^+$ T cells.[54–56] Previous studies in CD8 knockout and perforin knockout mice have demonstrated that $CD8^+$ T cells play a secondary role in the rejection of corneal allografts.[57,58] It was shown that delayed-type hypersensitivity, a $CD4^+$ T-cell–dependent immune response, and corneal transplant rejection in mice are highly correlated.[59,60] Whereas in keratoconus patients a significant increase of $\gamma\delta$-T cells on the ocular surface was shown,[61] the presence of $CD4^+$ or $CD8^+$ T cells was not yet reported. In addition, the recruitment of $CD4^+$ or $CD8^+$ T cells for the alkali burn and suture placement models was not yet reported. This finding is also reflected in our data, where only in the keratoplasty models $CD3^+CD4^+/CD8^+$ cells occur. Interestingly, $CD4^+$ T cells were significantly less recruited in LR-KPL in total as well as in the central and peripheral cornea. The $CD8^+$ T-cell frequency was generally lower and did not change between high- and low-risk settings, except in the center. It was shown that corneal grafts placed in eyes with a low-risk rejection hardly induce direct alloreactive $CD4^+$ or $CD8^+$ T cells,[62] whereas grafts placed in high-risk beds strongly induce direct alloreactive $CD4^+$ and $CD8^+$ T effector cells.[63] Here, we show for the first time a direct, quantitative comparison of corneal $CD4^+$ and $CD8^+$ T cells in the cornea after HR-KPL and LR-KPL.

Moreover, it is well-known that lymph nodes play a crucial role in corneal alloimmunization and graft rejection.[64,65] We showed in this study that activated macrophages and DCs expressing MHC II were significantly increased in HR-KPL and LR-KPL (Figs. 5A, 5D). In the dLNs, activation of T cells requires first signal stimulation, that is, MHC II expressed by APCs.[66] In the allogeneic keratoplasty model, much more activated APCs could cause a more intense adaptive immune response.

HR-KPL and LR-KPL induced considerably more neutrophil, macrophage, DCs, MHC II^+ cell, and T-cell cornea invasion compared with than all other groups. Moreover, HR-KPL has significantly more corneal MHC II^+ cells and $CD4^+$ T cells than LR-KPL. An increase in activated APCs and $CD4^+$ T cells, which are closely associated with the immune response to corneal transplantation, explain the cellular mechanisms underlying the high rejection rate in high-risk corneal transplants.

In this study, we only compared the corneal neovascularization and immune cell infiltration at one time point after different corneal injuries. Corneal BVs, LVs, and immune cells presumably change over time after the initial insult.[67] Moreover, the difference in molecular response pattern and the local cytokine milieu in different injury models leading to high-risk settings is also a direction for our future research; it will validate these differences in human tissue samples. Nevertheless, in this study, we demonstrate for the first time significant variation in the immune cell composition both in the recipient bed and the lymphoid organs in various high-risk settings. This is of high clinical relevance because patients currently receive similar therapies mainly consisting of the application of corticosteroids.[68] These disease-specific neovascularization and immune cells pattern ("signatures") may have a different impact on immune responses after subsequent transplantation. Thus, they will establish more personalized treatment algorithms for high-risk patients depending on their individual preexisting pathologies in the future.

In conclusion, different types of corneal injury cause different types and degrees of neovascularization and

Investigative Ophthalmology & Visual Science

immune cell infiltration. These novel hemangiogenic and lymphangiogenic and immune cell signatures will have to be studied further with respect to their impact on subsequent high-risk corneal graft survival. Our results will help to pave the way toward more disease-specific and personalized anti(lymph)angiogenic and immunomodulatory treatment strategies to promote high-risk corneal graft survival in the future.[69,70]

Acknowledgments

The authors thank Gabriele Braun for very valuable help. We also thank Maria Notara for English editing.

Funding Statement: German Research Foundation (DFG) FOR2240 "(Lymph)angiogenesis and Cellular Immunity in Inflammatory Diseases of the Eye," (www.for2240.de). Grant number: Cu 47/4-2, Cu 47/6-1, Cu 47/9-1, Cu 47/15-1 (CC), BO4489/1-1, BO4489/1-2, BO4489/3-1 (FB); BMBF KS (01KG2127; CC); EU COST Aniridia (CC; www.aniridia-net.eu); EU Horizon 2020 ARREST BLINDNESS (CC; www.arrestblindness.eu); Center for Molecular Medicine Cologne, University of Cologne (FB, CC; www.cmmc-uni-koeln.de/home/); China Scholarship Council (WZ; csc.edu.cn).

Disclosure: **W. Zhang**, None; **A. Schönberg**, None; **F. Bassett**, None; **K. Hadrian**, None; **D. Hos**, None; **M. Becker**, None; **F. Bock**, None; **C. Cursiefen**, None

References

1. Wang S, Ghezzi CE, Gomes R, Pollard RE, Funderburgh JL, Kaplan DL. In vitro 3D corneal tissue model with epithelium, stroma, and innervation. *Biomaterials.* 2017;112:1–9.
2. Streilein JW. Ocular immune privilege: Therapeutic opportunities from an experiment of nature. *Nat Rev Immunol.* 2003;3(11):879–889.
3. Cursiefen C, Chen L, Saint-Geniez M, et al. Nonvascular VEGF receptor 3 expression by corneal epithelium maintains avascularity and vision. *Proc Natl Acad Sci USA.* 2006;103(30):11405–11410.
4. Flockerzi E, Maier P, Böhringer D, et al. Trends in corneal transplantation from 2001 to 2016 in Germany: A report of the DOG-section cornea and its keratoplasty registry. *Am J Ophthalmol.* 2018;188:91–98.
5. Matthaei M, Sandhaeger H, Hermel M, et al. Changing indications in penetrating keratoplasty: A systematic review of 34 years of global reporting. *Transplantation.* 2017;101(6):1387–1399.
6. Williams KA, Esterman AJ, Bartlett C, Holland H, Hornsby NB, Coster DJ. How effective is penetrating corneal transplantation? Factors influencing long-term outcome in multivariate analysis. *Transplantation.* 2006;81(6):896–901.
7. Maguire MG, Stark WJ, Gottsch JD, et al. Risk factors for corneal graft failure and rejection in the collaborative corneal transplantation studies. Collaborative Corneal Transplantation Studies Research Group. *Ophthalmology.* 1994;101(9):1536–1547.
8. Bachmann B, Taylor RS, Cursiefen C. Corneal neovascularization as a risk factor for graft failure and rejection after keratoplasty: An evidence-based meta-analysis. *Ophthalmology.* 2010;117(7):1300–1305.e1307.
9. Di Zazzo A, Kheirkhah A, Abud TB, Goyal S, Dana R. Management of high-risk corneal transplantation. *Surv Ophthalmol.* 2017;62(6):816–827.
10. Singh RB, Marmalidou A, Amouzegar A, Chen Y, Dana R. Animal models of high-risk corneal transplantation: A comprehensive review. *Exp Eye Res.* 2020;198:108152.
11. Coster DJ, Williams KA. The impact of corneal allograft rejection on the long-term outcome of corneal transplantation. *Am J Ophthalmol.* 2005;140(6):1112–1122.
12. Chen L, Hamrah P, Cursiefen C, et al. Vascular endothelial growth factor receptor-3 mediates induction of corneal alloimmunity. *Nat Med.* 2004;10(8):813–815.
13. Hos D, Bukowiecki A, Horstmann J, et al. Transient ingrowth of lymphatic vessels into the physiologically avascular cornea regulates corneal edema and transparency. *Sci Rep.* 2017;7(1):7227.
14. Anderson C, Zhou Q, Wang S. An alkali-burn injury model of corneal neovascularization in the mouse. *J Vis Exp.* 2014(86):51159.
15. Qazi Y, Hamrah P. Corneal allograft rejection: Immunopathogenesis to therapeutics. *J Clin Cell Immunol.* 2013;11:2013.
16. Cursiefen C, Chen L, Borges LP, et al. VEGF-A stimulates lymphangiogenesis and hemangiogenesis in inflammatory neovascularization via macrophage recruitment. *J Clin Invest.* 2004;113(7):1040–1050.
17. Cursiefen C, Cao J, Chen L, et al. Inhibition of hemangiogenesis and lymphangiogenesis after normal-risk corneal transplantation by neutralizing VEGF promotes graft survival. *Invest Ophthalmol Vis Sci.* 2004;45(8):2666–2673.
18. Lamy R, Wolf M, Bispo C, et al. Characterization of recruited mononuclear phagocytes following corneal chemical injury. *Int J Mol Sci.* 2022;23(5):2574.
19. Bock F, Onderka J, Dietrich T, et al. Bevacizumab as a potent inhibitor of inflammatory corneal angiogenesis and lymphangiogenesis. *Invest Ophthalmol Vis Sci.* 2007;48(6):2545–2552.
20. Hos D, Bucher F, Regenfuss B, et al. IL-10 indirectly regulates corneal lymphangiogenesis and resolution of inflammation via macrophages. *Am J Pathol.* 2016;186(1):159–171.
21. Bock F, Onderka J, Hos D, Horn F, Martus P, Cursiefen C. Improved semiautomatic method for morphometry of angiogenesis and lymphangiogenesis in corneal flatmounts. *Exp Eye Res.* 2008;87(5):462–470.
22. Salabarria AC, Koch M, Schönberg A, et al. Topical VEGF-C/D inhibition prevents lymphatic vessel ingrowth into cornea but does not improve corneal graft survival. *J Clin Med.* 2020;9(5):1270.
23. Salabarria AC, Braun G, Heykants M, et al. Local VEGF-A blockade modulates the microenvironment of the corneal graft bed. *Am J Transplant.* 2019;19(9):2446–2456.
24. Dietrich T, Bock F, Yuen D, et al. Cutting edge: Lymphatic vessels, not blood vessels, primarily mediate immune rejections after transplantation. *J Immunol.* 2010;184(2):535–539.
25. Wang J. Neutrophils in tissue injury and repair. *Cell Tissue Res.* 2018;371(3):531–539.
26. Elbasiony E, Mittal SK, Foulsham W, Cho W, Chauhan SK. Epithelium-derived IL-33 activates mast cells to initiate neutrophil recruitment following corneal injury. *Ocular Surf.* 2020;18(4):633–640.
27. Kiesewetter A, Cursiefen C, Eming SA, Hos D. Phase-specific functions of macrophages determine injury-mediated corneal hem- and lymphangiogenesis. *Sci Rep.* 2019;9(1):308.
28. Hamrah P, Liu Y, Zhang Q, Dana MR. The corneal stroma is endowed with a significant number of resident dendritic cells. *Invest Ophthalmol Vis Sci.* 2003;44(2):581–589.
29. Willrodt AH, Salabarria AC, Schineis P, et al. ALCAM mediates DC migration through afferent lymphatics and promotes allospecific immune reactions. *Front Immunol.* 2019;10:759.
30. Peckert-Maier K, Schönberg A, Wild AB, et al. Pre-incubation of corneal donor tissue with sCD83 improves graft survival via the induction of alternatively activated

macrophages and tolerogenic dendritic cells. *Am J Transplant.* 2022;22(2):438–454.
31. Colby K, Adamis A. Prevalence of corneal vascularization in a general eye service population. *Invest Ophthalmol Vis Sci.* 1996;37(3):2734–2734.
32. Lee P, Wang CC, Adamis AP. Ocular neovascularization: An epidemiologic review. *Surv Ophthalmol.* 1998;43(3):245–269.
33. Cursiefen C, Schlötzer-Schrehardt U, Küchle M, et al. Lymphatic vessels in vascularized human corneas: Immunohistochemical investigation using LYVE-1 and podoplanin. *Invest Ophthalmol Vis Sci.* 2002;43(7):2127–2135.
34. Cursiefen C, Martus P, Nguyen NX, Langenbucher A, Seitz B, Küchle M. Corneal neovascularization after nonmechanical versus mechanical corneal trephination for non-high-risk keratoplasty. *Cornea.* 2002;21(7):648–652.
35. Cursiefen C, Chen L, Dana MR, Streilein JW. Corneal lymphangiogenesis: Evidence, mechanisms, and implications for corneal transplant immunology. *Cornea.* 2003;22(3):273–281.
36. Hos D, Cursiefen C. Lymphatic vessels in the development of tissue and organ rejection. *Adv Anat Embryol Cell Biol.* 2014;214:119–141.
37. Dana MR. Angiogenesis and lymphangiogenesis-implications for corneal immunity. *Semin Ophthalmol.* 2006;21(1):19–22.
38. Perlman JI. Ocular disease: Mechanisms and management. *JAMA.* 2011;306(1):101–101.
39. Hamrah P, Huq SO, Liu Y, Zhang Q, Dana MR. Corneal immunity is mediated by heterogeneous population of antigen-presenting cells. *J Leukoc Biol.* 2003;74(2):172–178.
40. Brissette-Storkus CS, Reynolds SM, Lepisto AJ, Hendricks RL. Identification of a novel macrophage population in the normal mouse corneal stroma. *Invest Ophthalmol Vis Sci.* 2002;43(7):2264–2271.
41. Bukowiecki A, Hos D, Cursiefen C, Eming SA. Wound-healing studies in cornea and skin: Parallels, differences and opportunities. *Int J Mol Sci.* 2017;18(6):1257.
42. Hong JW, Liu JJ, Lee JS, et al. Proinflammatory chemokine induction in keratocytes and inflammatory cell infiltration into the cornea. *Invest Ophthalmol Vis Sci.* 2001;42(12):2795–2803.
43. Ebihara N, Matsuda A, Nakamura S, Matsuda H, Murakami A. Role of the IL-6 classic- and trans-signaling pathways in corneal sterile inflammation and wound healing. *Invest Ophthalmol Vis Sci.* 2011;52(12):8549–8557.
44. Sotozono C, He J, Matsumoto Y, Kita M, Imanishi J, Kinoshita S. Cytokine expression in the alkali-burned cornea. *Curr Eye Res.* 1997;16(7):670–676.
45. Li Z, Burns AR, Smith CW. Two waves of neutrophil emigration in response to corneal epithelial abrasion: Distinct adhesion molecule requirements. *Invest Ophthalmol Vis Sci.* 2006;47(5):1947–1955.
46. O'Brien TP, Li Q, Ashraf MF, Matteson DM, Stark WJ, Chan CC. Inflammatory response in the early stages of wound healing after excimer laser keratectomy. *Arch Ophthalmol.* 1998;116(11):1470–1474.
47. Tran MT, Tellaetxe-Isusi M, Elner V, Strieter RM, Lausch RN, Oakes JE. Proinflammatory cytokines induce RANTES and MCP-1 synthesis in human corneal keratocytes but not in corneal epithelial cells. Beta-chemokine synthesis in corneal cells. *Invest Ophthalmol Vis Sci.* 1996;37(6):987–996.
48. Marshall JS, Warrington R, Watson W, Kim HL. An introduction to immunology and immunopathology. *Allergy Asthma Clin Immunol.* 2018;14(Suppl 2):49.
49. Koudouna E, Okumura N, Okazaki Y, et al. Immune cells on the corneal endothelium of an allogeneic corneal transplantation rabbit model. *Invest Ophthalmol Vis Sci.* 2017;58(1):242–251.
50. Yamada J, Hamuro J, Fukushima A, et al. MHC-matched corneal allograft rejection in an IFN-gamma/IL-17-independent manner in C57BL/6 mice. *Invest Ophthalmol Vis Sci.* 2009;50(5):2139–2146.
51. Scozzi D, Ibrahim M, Menna C, Krupnick AS, Kreisel D, Gelman AE. The role of neutrophils in transplanted organs. *Am J Transplant.* 2017;17(2):328–335.
52. Banchereau J, Steinman RM. Dendritic cells and the control of immunity. *Nature.* 1998;392(6673):245–252.
53. Kuffová L, Netuková M, Duncan L, Porter A, Stockinger B, Forrester JV. Cross presentation of antigen on MHC class II via the draining lymph node after corneal transplantation in mice. *J Immunol.* 2008;180(3):1353–1361.
54. Williams KA, White MA, Ash JK, Coster DJ. Leukocytes in the graft bed associated with corneal graft failure. Analysis by immunohistology and actuarial graft survival. *Ophthalmology.* 1989;96(1):38–44.
55. Larkin DF, Calder VL, Lightman SL. Identification and characterization of cells infiltrating the graft and aqueous humour in rat corneal allograft rejection. *Clin Exp Immunol.* 1997;107(2):381–391.
56. Pepose JS, Nestor MS, Gardner KM, Foos RY, Pettit TH. Composition of cellular infiltrates in rejected human corneal allografts. *Graefes Arch Clin Exp Ophthalmol.* 1985;222(3):128–133.
57. Yamada J, Ksander BR, Streilein JW. Cytotoxic T cells play no essential role in acute rejection of orthotopic corneal allografts in mice. *Invest Ophthalmol Vis Sci.* 2001;42(2):386–392.
58. Hegde S, Niederkorn JY. The role of cytotoxic T lymphocytes in corneal allograft rejection. *Invest Ophthalmol Vis Sci.* 2000;41(11):3341–3347.
59. Joo CK, Pepose JS, Stuart PM. T-cell mediated responses in a murine model of orthotopic corneal transplantation. *Invest Ophthalmol Vis Sci.* 1995;36(8):1530–1540.
60. Sonoda Y, Streilein JW. Impaired cell-mediated immunity in mice bearing healthy orthotopic corneal allografts. *J Immunol.* 1993;150(5):1727–1734.
61. D'Souza S, Nair AP, Sahu GR, et al. Keratoconus patients exhibit a distinct ocular surface immune cell and inflammatory profile. *Sci Rep.* 2021;11(1):20891.
62. Sano Y, Streilein JW, Ksander BR. Detection of minor alloantigen-specific cytotoxic T cells after rejection of murine orthotopic corneal allografts: Evidence that graft antigens are recognized exclusively via the "indirect pathway". *Transplantation.* 1999;68(7):963–970.
63. Sano Y, Ksander BR, Streilein JW. Murine orthotopic corneal transplantation in high-risk eyes. Rejection is dictated primarily by weak rather than strong alloantigens. *Invest Ophthalmol Vis Sci.* 1997;38(6):1130–1138.
64. Yamagami S, Dana MR, Tsuru T. Draining lymph nodes play an essential role in alloimmunity generated in response to high-risk corneal transplantation. *Cornea.* 2002;21(4):405–409.
65. Yamagami S, Dana MR. The critical role of lymph nodes in corneal alloimmunization and graft rejection. *Invest Ophthalmol Vis Sci.* 2001;42(6):1293–1298.
66. Pilat N, Sayegh MH, Wekerle T. Costimulatory pathways in transplantation. *Semin Immunol.* 2011;23(4):293–303.
67. Shi W, Ming C, Liu J, Wang T, Gao H. Features of corneal neovascularization and lymphangiogenesis induced by different etiological factors in mice. *Graefes Arch Clin Exp Ophthalmol.* 2011;249(1):55–67.

Investigative Ophthalmology & Visual Science

68. Azevedo Magalhaes O, Shalaby Bardan A, Zarei-Ghanavati M, Liu C. Literature review and suggested protocol for prevention and treatment of corneal graft rejection. *Eye (London, England)*. 2020;34(3):442–450.
69. Cursiefen C, Hos D. Cutting edge: Novel treatment options targeting corneal neovascularization to improve high-risk corneal graft survival. *Cornea*. 2021;40(12):1512–1518.
70. Cursiefen C, Cordeiro F, Cunha-Vaz J, Wheeler-Schilling T, Scholl HPN. Unmet needs in ophthalmology: A European Vision Institute-consensus roadmap 2019-2025. *Ophthalm Res*. 2019;62(3):123–133.

Investigative Ophthalmology & Visual Science